

Effect of Sweep Angle and Drag on the Flutter Speed of Hydrofoils

J. Mahig*

University of Florida, Gainesville, Fla.

A determination is made of the effect on flutter frequency and speed on variations in the drag coefficient and sweep angle. The strip method of analysis is used with wing stiffness being estimated through strength of material analyses. The drag and lift slope coefficient are estimated to compare with experimental data obtained by T. T. Huang. These estimates obtain results which are shown to provide more favorable comparisons with various experiments conducted by him, than could be obtained heretofore. Although comparisons obtained are considered favorable, trends in the data for increasing slope angles are not completely satisfactory which indicates that a further refinement in the theory is still required. Discussion of the possible source for these trends and the limits of applicability of this approach are considered.

Nomenclature

- a = nondimensional distance of elastic areas from midchord
- \bar{a} = unwetted length of hydrofoil
- b = wing half chord (measured perpendicular to leading edge)
- C_D = drag coefficient
- C_L = lift coefficient
- EI = longitudinal bending stiffness of foil
- h = total lateral displacement of elastic axis
- h_i = component of lateral displacement at midchord point (pure bending mode)
- \dot{h} = lateral velocity of midchord point (pure bending mode)
- JG = torsional stiffness of foil
- l = total length of foil
- \bar{l} = wave length of harmonic gusts
- M = bending moment
- m = mass/unit length along leading edge
- v = stream velocity, in./sec
- V = shear force
- x_α = nondimensional distance of c.g. from elastic axis measured in half chords (positive for position of c.g. behind elastic axis)
- α = rotational displacement (radians)
- β = defined as \bar{a}/l
- γ_α = radius of gyration relative to elastic axis
- γ = sweep angle
- ξ = see Fig. 1
- ζ = inverse reduced frequency, $v/\omega b$
- ρ = density of test medium, lb-sec/in.
- μ = ratio of structural mass to mass of surrounding cylinder of water
- ω = flutter frequency

Introduction

ALTHOUGH the phenomenon of aircraft wing flutter is so well understood that the method of prediction is considered classical, this same method has been shown to be insufficient for the consistent prediction of the onset of the hydrofoil flutter phenomenon. As a result, in recent years much interest has been evident in defining the significant parameters and determining the precision with which they should be measured so as to accurately estimate the flutter speed of hydrofoils.

Among the studies of this problem is the work of Dugundji and Ghareeb,¹ who showed that the mode shape of flutter changes from that of a standing wave type flutter for high mass ratios to a traveling wave type for low. Yates² initiated a modified development of the strip

method by employing arbitrary spanwise distribution of the lift curve slope and c.p. location in order to gain a more satisfactory comparison with test results.

Other investigators have attempted to utilize the full application of lifting surface theories in solution of the problem. Such a procedure has been proposed by Rowe.³ His method allows some variation in the satisfaction of the Kutta condition and inherently generates data on the lift curve slope and c.p. location.

Abramson and Chu⁴ obtained encouraging results from their analysis which is based on strip theory. The analysis involves modifications to account for the Kutta condition and variation of the location of the lift curve slope and c.p. location. The application of these conclusions were then used to obtain a conservative flutter speed for the SWRI flutter model as a case in point, and at the same time showed the profound influence on the flutter speed caused by changes in the c.p. location and by variations in the lift curve slope along the wing. Mahig,⁵ using the strip theory, showed that not only did the lift curve slope affect the flutter speed but that the drag forces which have heretofore been neglected in the literature had an even more profound effect.

Although the sensitivity of the flutter speed to variations in the drag coefficient, c.p. location, and lift curve slope have been studied, the effect of sweep back concurrent with the effect of the drag forces has not been considered analytically by anyone. The analysis presented below does this, and as a result, makes possible a more detailed comparison of theoretical calculations with the experimental results obtained by T. T. Huang.⁶

Methodology

The analysis presented below assumes that strip analysis is sufficient, that structural damping can be neglected, and that although μ is low for the hydrofoil considered, the mode of vibration may be assumed to be a coupled torsional bending standing wave with a superimposed bending mode. In addition, the c.p. location is assumed at the quarter chord point and the value of the lift curve slope is considered constant along the wing.

The fluctuating lift generated by the coupled torsional bending mode has been obtained through the use of a Kemp and Sears model.⁷ Using nomenclature consistent with that defined in Fig. 1, the fluctuating lift may be shown to be given as

$$\Delta L = 2\pi\rho v u_0 \exp(i\omega t) S(\zeta^{-1}) \quad (1)$$

Received September 13, 1972; revision received February 20, 1973.

Index categories: Marine Vessel Trajectories, Stability and Control; Marine Vessel Vibration.

*Associate Professor, Department of Mechanical Engineering.

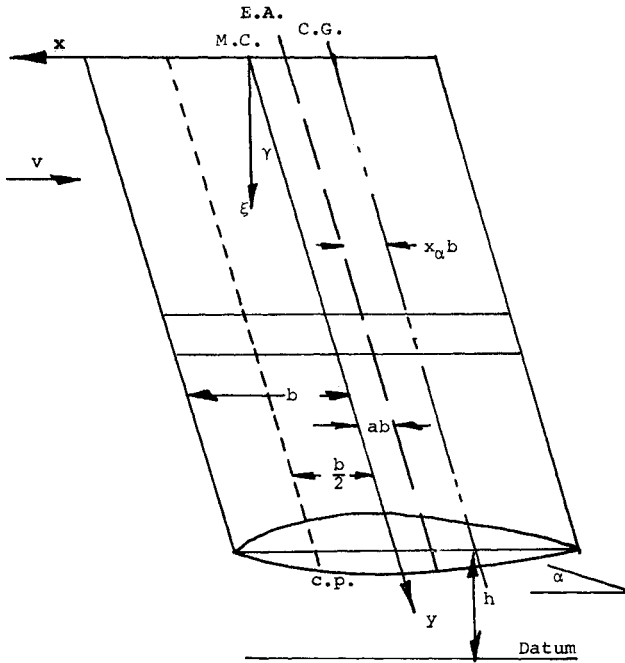


Fig. 1 Schematic of the hydrofoil showing the location of the coordinate system and significant parameters.

where the harmonic gust u may be given as

$$u = u_0 \exp[i\omega(t + x/v)]$$

and

$$\xi^{-1} = (2\pi v/\bar{l})/v = 2\pi/\bar{l}$$

when the semichord is one.

The quasi-steady lift developed by the associated pure bending mode due to a transverse gust whose velocity component remains constant along the entire chord may be given as

$$\Delta L = \partial C_L / \partial \alpha (u/v) \rho v^2 b \Delta \xi \quad (3)$$

for a foil with lift coefficient C_L . It can be shown that this lift may be expressed in terms of the foils coordinate system as follows:

$$\Delta L = \partial C_L / \partial \alpha (\alpha - \bar{h}/v) \rho v^2 b \Delta \xi \quad (4)$$

where \bar{h} is the velocity of the midchord point due to the pure bending mode.

The contribution of the drag forces to the increase in torque over the differential element may be calculated from the element shown in Fig. 2. The change in torque is measured about the elastic axis with the center of pressure located at the quarter chord point.

The additional torque, exerted on the element due to drag force, is considered to be made of two components: one due to the total drag forces developed over the section of the wing outboard of the element, and the other is due to the component of the drag force over the element itself. The former torque can be shown to be

$$\Delta T = C_D \rho v^2 b (l \cos \gamma - \xi) \frac{\partial}{\partial y} [h + (a + 0.5)\alpha b] \Delta \xi \quad (5)$$

where l is the length of the wing. The latter torque evaluated about the elastic axis may be given as

$$\Delta T = C_D \rho v^2 b (a + 0.5) \quad (6)^\dagger$$

[†]For a c.p. location at the quarter chord.

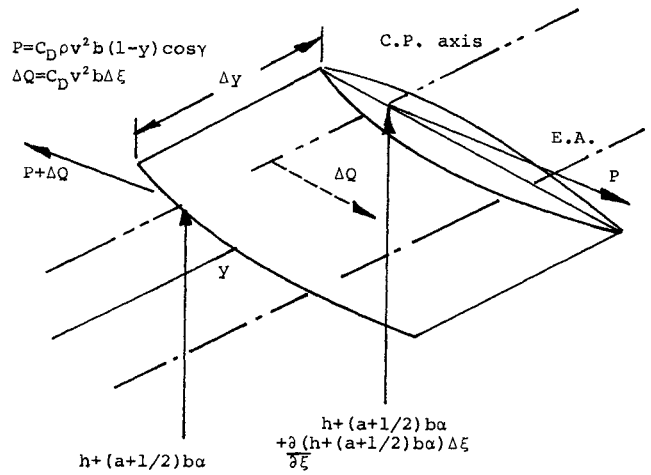


Fig. 2 Drag force element; the forces shown acting on the element are only those due to the drag forces.

Element Equilibrium

An exact representation of the torsional and bending stiffness of a swept wing cannot be accomplished using only strength of material concepts, since it is necessary to neglect the corner elements at either end of the wing; nonetheless, one may expect that excellent results should be obtainable for modest sweep angles. For convenience, the equations of motion are developed for two separate free body elements. One of these elements is cut along the direction of flow as shown in Fig. 3, and the other is cut perpendicular to the leading edge of the wing as shown in Fig. 4.

Let us first consider the element cut along the flow path (Fig. 3) and determine the torsional equilibrium equations from that element

$$J \ddot{\alpha} = - \frac{\partial T}{\partial \xi} + \frac{\sin \gamma}{\cos \gamma} (V - \frac{\partial M}{\partial y}) + \frac{\partial F_v}{\partial \xi} (a + 0.5) \quad (7)$$

where F_v is the lateral force developed normal to the element due to the fluid flow. When the transverse equilibrium equation is applied to this element, the following relationship is obtained.

$$(\rho \pi b^2 + m) \ddot{h} - \ddot{\alpha} (m x_{\alpha} b - \rho \pi b^2 a b) = \frac{\partial F_v}{\partial \xi} - \frac{\partial V}{\partial \xi} \quad (8)$$

From the bending element shown in Fig. 4, one can obtain

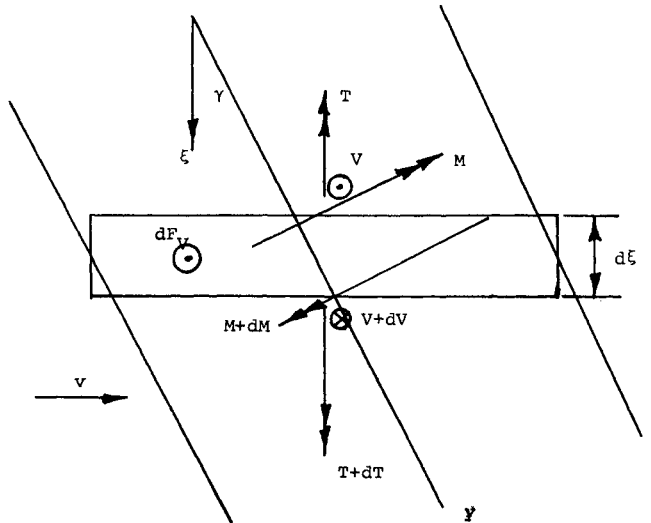


Fig. 3 Torsional element, that element cut from wing parallel to the velocity of flow.

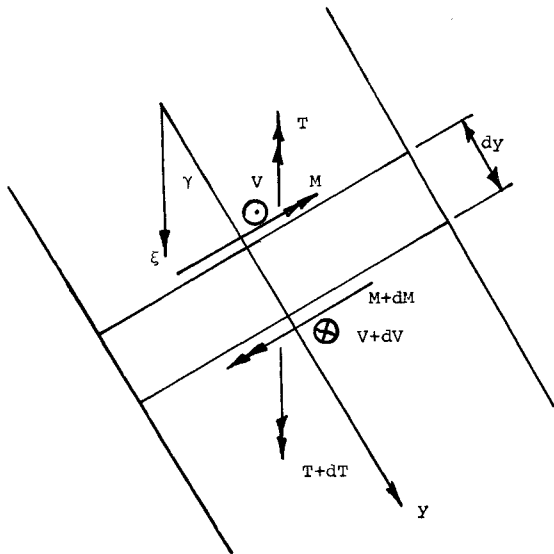


Fig. 4 Bending element, that element cut from wing perpendicular to leading edge.

the relation

$$\frac{\partial T}{\partial \xi} \sin \gamma \cos \gamma = V - \frac{\partial M}{\partial y} \quad (9)$$

By substituting Eq. (9) into Eq. (7), it is found that the torsional equation can be expressed as

$$m \ddot{\alpha} \gamma_a^2 b + \dot{h} m x_a b + \rho \pi b^3 (\ddot{\alpha} b (.125 + a^2) - a \dot{h}) = - \frac{\partial T}{\partial \xi} \cos^2 \gamma + \frac{\partial F_v}{\partial \xi} (a + 0.5) \quad (10)$$

since $M = EIh''$, it can be shown that

$$\rho \pi b^2 (\ddot{h} - a b \ddot{\alpha}) + m (\ddot{h} - x_a \ddot{\alpha}) = \frac{\partial F_v}{\partial \xi} - \frac{\partial^2 T}{\partial \xi^2} \sin \gamma \cos \gamma - \frac{EIh''''}{\cos \gamma} \quad (11)$$

where

$$\frac{\partial^2 T}{\partial \xi^2} = \frac{\partial G}{\cos^3 \gamma} \frac{\partial^3 \alpha}{\partial y^3}$$

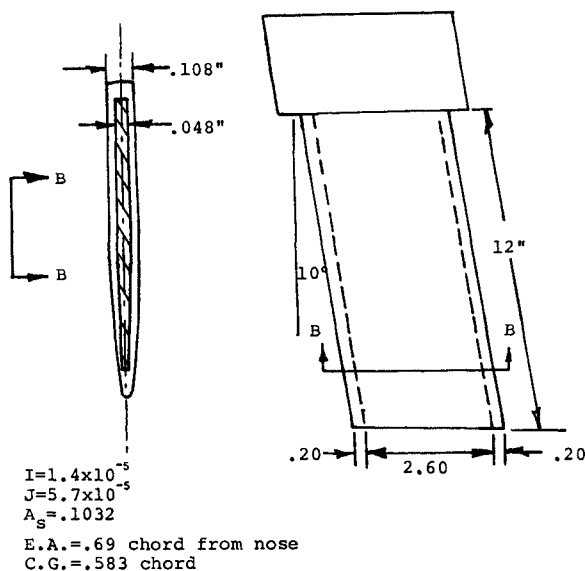


Fig. 5 T. T. Huang's foil used in the experiments at Hydro-nautics Inc.

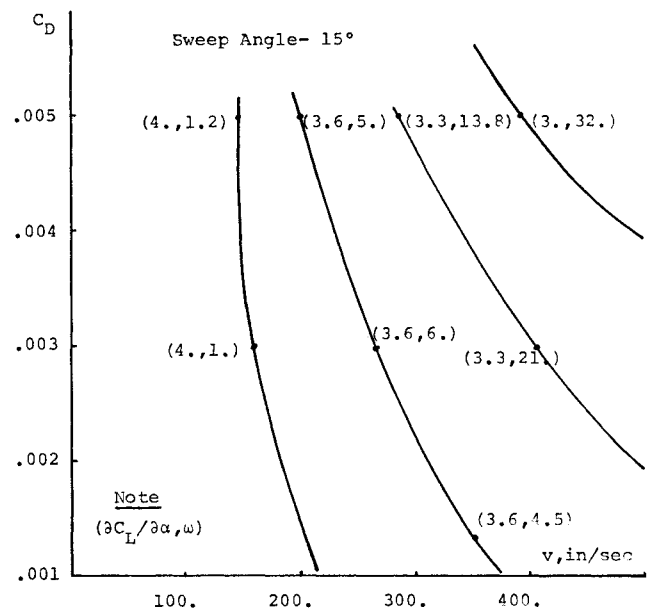


Fig. 6 Coefficient of drag vs flutter velocity and frequency for various values of $\partial C_L / \partial \alpha$, for a sweep angle of 15°.

The complete form of the equations of motion which explicitly includes the fluid forces, may be expressed as

$$m \ddot{\alpha} \gamma_a^2 b + \rho \pi b^4 \ddot{\alpha} (.125 + a^2) + \dot{h} (m x_a b - \rho \pi b^3 a) = b (1/2 + a) \rho \pi b^2 \dot{\alpha} v - \frac{\partial^2 \alpha}{\partial y^2} JG - 4 \pi \rho v S (\zeta^{-1}) \dot{h}_1 (a + 0.5) \zeta w b + \frac{\partial C_L}{\partial \alpha} (\alpha - \dot{h}/v) v^2 \rho b (a + 1/2) b + \frac{\partial}{\partial y} [(a + 1/2) b \alpha + h] C_D \cdot \rho v^2 b (l \cos \gamma - \xi) + C_D \rho v^2 b^2 (1/2 + a) \alpha \quad (12)$$

where all terms such as m , b , a etc., are defined for the torsional element as shown in Fig. 1. The equations of motion of the bending elements may be expressed as

$$\ddot{h} (m + \rho \pi b^2) - \ddot{\alpha} (m x_a b - \rho \pi b^3 a) = -EI / \cos \gamma h'''' - JG \sin \gamma / \cos^2 \gamma \partial^3 \alpha / \partial y^3 + \rho \pi b^2 \alpha v - 4 \pi \rho v S (\zeta^{-1}) \dot{h}_1 \zeta w + 2 C_L / \partial \alpha (\alpha - \dot{h}/v) v^2 \rho b \quad (13)$$

where m , b , a are as defined for the bending element; that is, all measurements are taken perpendicular to the leading edge.

The displacements α , h_1 , h are assumed to be given as follows:

$$\begin{aligned} \alpha &= A_1 Y \exp(i \omega t) \\ h_1 &= -b \zeta i A_1 Y \exp(i \omega t) \\ h &= -A_2 i Y \exp(i \omega t) \end{aligned} \quad (14)$$

where Y is the assumed static deflection of a uniformly loaded cantilever beam and A_1 and A_2 are the unknown amplitude of motion. This deflection curve may be shown to be given as

$$Y(y) = A (l^2 y^2 / 4 - l y^3 / 6 + y^4 / 24) \quad (15)$$

Upon substitution of the assumed displacements, α , h_1 , h into Eqs. (12 and 13) and applying the usual strip analysis procedure, the following set of nondimensionalized

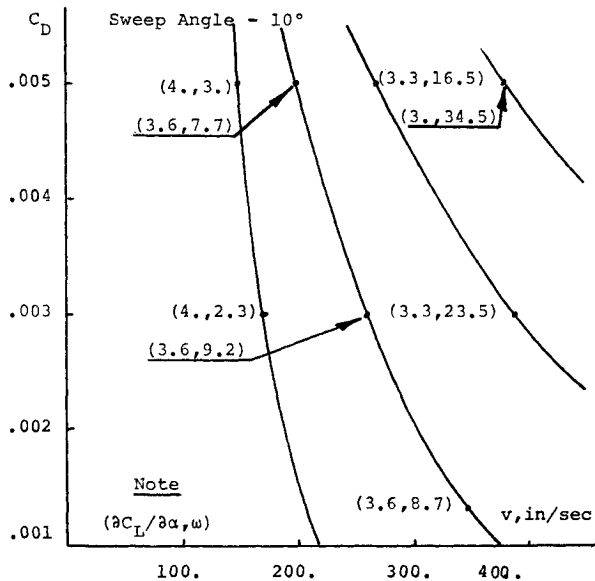


Fig. 7 Coefficient of drag vs flutter velocity and frequency for various values of $\partial C_L/\partial \alpha$, for a sweep angle of 10° .

equations may be obtained after some algebraic manipulations

$$\begin{aligned} & [-w^2 \gamma_\alpha^2 - w^2/\mu(0.125 + a^2) - i w v / \mu b (0.5 + a) \psi \\ & + J G \bar{\psi} / m b^2 + 4 v \psi S(\xi^{-1}) (0.5 + a) \xi w / b^2 \mu + \partial C_L / \partial \alpha \alpha \psi v \\ & (0.5 + a) (-0.2 + a i / \xi) - (0.5 + a) C_D v^2 (\varphi + \psi) / \mu \pi b^2] A_1 \\ & + [-i w^2 / b (x_\alpha - a / \mu) + \partial C_L / \partial \alpha \psi v (0.5 + a) w / \mu b \pi \\ & + C_D \varphi v^2 i / \pi b^3 \mu] A_2 = 0 \end{aligned} \quad (16)$$

and

$$\begin{aligned} & [w^2 (x_\alpha - a / \mu) - i w v \psi / b \mu + 4 v \psi S(\xi^{-1}) \xi w / \mu b^2 \\ & - \partial G \tan \gamma \bar{\psi} / \cos \gamma + \partial C_L / \partial \alpha v \xi w \psi (-2. + a i / \xi) / \mu \pi b^2] A_1 \\ & + [\partial C_L / \partial \alpha \psi v w / \mu \pi b^2 - i E I \bar{\psi} / m b \cos \gamma] \end{aligned} \quad (17)$$

where a , b , J , m etc., are associated with the torsional element and

$$\beta = \bar{a} / l$$

$$\psi = 1. + \beta^2 250 (-0.0125 + \beta / 72. - \beta^2 / 144. + \beta^3 / 576. - \beta^4 / 5184)$$

$$\bar{\psi} = 0.75 / l^2$$

$$\bar{\bar{\psi}} = 12.5 / l^4$$

$$\varphi = (7.98 - 4.5 \beta^4 - 2.4 \beta^5 - 2.5 \beta^6) 0.1734 \cos \gamma$$

$$\bar{\bar{\bar{\psi}}} = -416 / l^3$$

The values of w and v which make the determinant of the system equal to zero are defined to be the flutter velocity and frequency.

Results

T. T. Huang published the results of a series of experiments on a hydrofoil which were conducted at Hydronautics Inc.⁶ This paper provides a carefully detailed breakdown of the physical parameters as well as the results obtained from a typical foil under widely varying conditions. The model tested had similar elastic properties and foil centers as the one used by Baird^{8,9} in his model tests of the E-Foil configuration which was then under consideration for the PGH by Code 6363, NAVSEC (formerly

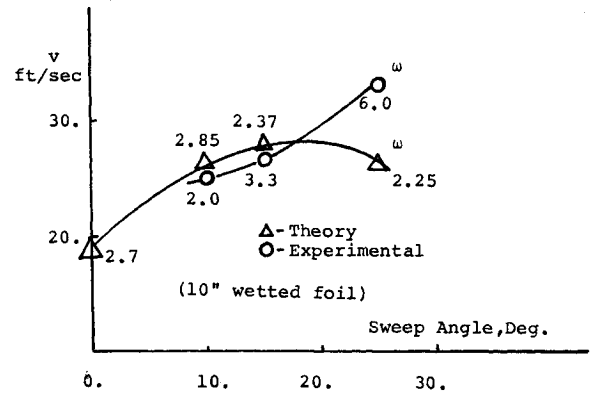


Fig. 8 Comparison of theoretical calculation with experimental results for various sweep angles of a hydrofoil with an unwetted length of 2 in.

Code 420, Bureau of Ships). Huang was able to conclude, as a result of preliminary tests, that his model had only negligible creep and internal damping as compared to Baird's. The quarter scale model used in his tests is shown in Fig. 5. However in this series of experiments neither the drag coefficient C_D nor the lift curve slope $\partial C_L / \partial \alpha$ were determined. Therefore, the values used in this study are only estimates. However, it is useful to obtain a measure of the consistency of the results obtained theoretically with some of those obtained from experiments actually carried out on a hydrofoil.

Plots of C_D vs divergence speed for differing sweep angles and lift curve slopes are shown in Figs. 6 and 7. There they show the marked variation in the divergence speed and frequency which occur with respect to variations in C_D and $\partial C_L / \partial \alpha$, the test results at a sweep angle of 10° for a depth of submergence of 10 in. were used. A careful analysis of Fig. 7 indicates that a foil with a C_D of 0.004 and a $\partial C_L / \partial \alpha$ of approximately 3.3 could be theoretically expected to have this same flutter speed and frequency.

In order to obtain a clearer insight into the degree of similarity of the results obtained theoretically and experimentally, Figs. 8 and 9 were plotted. These plots compare experimental results directly against theoretical calculations. Using the values of drag coefficient and lift curve slope developed above flutter speed vs sweep angle is plotted for two depths of submergence for comparison. In each figure the flutter speed for both experimental and theoretical results compare well to 20° sweep angles; however the flutter frequency appears to have an opposite trend.

Variation in system parameters and program checks did not discover how a significant change in the trend of the

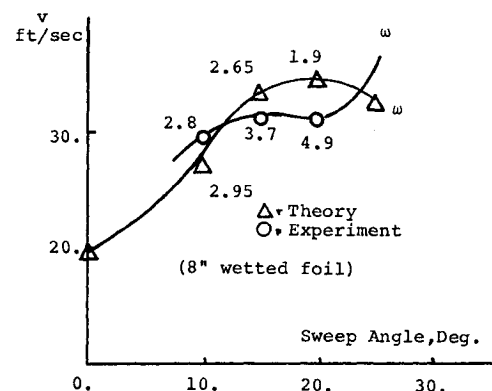


Fig. 9 Comparison of theoretical calculation with experimental results for various sweep angles for a hydrofoil with an unwetted length of 4 in.

frequency could be effected. At this writing it is felt that the significant fault may be in the strength of material approximation to wing stiffness. This type analysis implicitly assumes, as is usual in swept wing analysis, that a lateral force to the elastic axis produces no twisting. Since frequency appears to be the variable which has an undesirable trend, it is felt that the effect of fluid and inertial forces on wing twist should be considered for nonrectangular plan forms.

Conclusions

The theory presented appears to provide a reasonably consistent divergence speed up to sweep angles of 20°. However flutter frequency appears to have a trend which indicates further refinement is still necessary to completely describe the behavior of the foil. It is suggested in the text that it is felt that the strength of material approximation may be the cause of the flutter frequency variation determined, and the incorporation of wing twist due to lateral loads at the elastic axis of a foil, with a large sweep angle, may improve this frequency characteristic of this solution.

References

¹Dugundji, J. and Ghareeb, N., "Pure Bending Flutter of a

Swept Wing in a High Density, Low Speed Flow," Fluid Dynamics Research Group Rept. 64-1, March 1964, MIT, Cambridge, Mass.

²Yates, E. C., Jr., "Flutter Prediction at Low Mass Density Ratios with Application to the Finite-Span Subcavitating Hydrofoil," AIAA Paper 68-472, San Diego, Calif., 1968.

³Rowe, W. S., "Collocation Method for Calculating the Aerodynamic Pressure Distributions on a Lifting Surface Oscillating in Subsonic Compressible Flow," AIAA Symposium on Structural Dynamics and Aeroelasticity, AIAA, New York, 1965.

⁴Chu, W. and Abramson, N., "Further Calculations of the Flutter Speed of a Fully Submerged Subcavitating Hydrofoil," *Journal of Hydraulics*, Vol. 3, No. 4, Oct. 1969, pp. 168-174.

⁵Mahig, J., "Theory for the Determination of the Flutter Speed of a Class of Hydrofoils," *Journal of Engineering for Industry*, Vol. 94, Ser. B, No. 1, Feb. 1972, pp. 76-80.

⁶Huang, T. T., "Experimental Study of a Low Modulus Flutter Strut for a Hydrofoil System," *Journal of Hydraulics*, Vol. 2, No. 4, Oct. 1968, p. 198.

⁷Kemp, N. H. and Sears, W. R., "The Unsteady Forces Due to Viscous Wakes in Turbomachines," *Journal of Aeronautical Sciences*, Vol. 22, 1955, pp. 478-483.

⁸Baird, E. F., Squires, C. E., Jr., et al., "Investigation of Hydrofoil Flutter," Final Rept. DA10-480-3, Feb. 1962, Grumman Aircraft Engineering Corp, Bethpage, N.Y.

⁹Baird, E. F., Squires, C. E., Jr., and Caporali, R. L., "An Experimental and Theoretical Investigation of Hydrofoil Flutter," *Aerospace Engineering*, Vol. 21, No. 2, Feb. 1962, pp. 34-41.

JULY 1973

J. HYDRONAUTICS

VOL. 7, NO. 3

Impressed-Current Cathodic Protection of Aluminum-Hulled Craft

Boyce E. Miller* and Harvey P. Hack*

Naval Ship Research and Development Center, Annapolis, Md.

Overprotection is a major problem accompanying cathodic protection of aluminum-hulled craft. Investigations were conducted concerning the protection and overprotection of aluminum under various conditions of galvanic coupling, seawater velocities and dilutions, dielectric shield materials, lengths of exposure and influence of seawater location. Overprotection was found to occur above -1500 mv, the exact value depending on seawater velocity and other conditions. The corrosion resulting from overprotection was severe, making imperative a protection system design which eliminates the possibility of accidental overprotection. Data is presented which can aid in the design of a reliable protection system.

ALUMINUM alloys of the 5000-series are used for the hulls of hydrofoils, surface effect ships, and other weight-critical craft. While these alloys have good inherent resistance to corrosion in seawater, they are subject to accelerated attack if electrically connected to other structural alloys. The galvanic effect of coupling dissimilar metals in this electrolyte results in accelerated attack of the anodic member of the couple. Aluminum alloys are anodic to copper, nickel, and titanium alloys, steels, and any other common structural materials used for propellers, hydrofoil struts and foils, and seawater systems. In addition, metal barges or docks which might be accidentally coupled to an aluminum-hulled craft through a gangway or wire rope may also be constructed of these materials.

Use of a "protective" coating on the anodic alloy is likely to be more harmful than beneficial. Since some flaws or breaks in the coating are probable, the coating only serves to reduce the effective anodic area of the imperfections, leading to rapid attack in localized areas. Although coating of the cathodic materials is the recommended approach to reduce the galvanic current acting on the anodic material, this is not practical on aluminum craft where many of the other alloys encountered are in parts not suitable for coatings. Also, the aluminum hull should be coated for fouling resistance. For these reasons a cathodic protection system is required.

Several types of cathodic protection systems have been used on aluminum ships including zinc anodes, magnesium anodes, sprayed zinc coatings, and impressed-current systems. This note concerns the use of impressed-current systems such as illustrated in Fig. 1. A varying potential is applied between the hull and hull-mounted anodes in order to keep the hull at a constant potential relative to a Ag-AgCl reference cell. Two cells, several inches across, are usually located in the hull, well away

Received July 10, 1972; also presented as Paper 72-593 at the AIAA/SNAME/USN Advanced Marine Vehicles Meeting, Annapolis, Md., July 17-19, 1972; revision received March 22, 1973.

Index categories: Marine Surface Vessel Systems; Corrosion/Erosion of Marine Materials.

* Research Metallurgist.